

The Role of Mixed Graphene/Carbon Nanotubes on the Coating Performance of G/CNTs/Epoxy Resin Nanocomposites.

Mahmoud A. Hussein^{1,3,*}, Bahaa M. Abu-Zied^{1,2,3}, Abdullah M. Asiri^{1,2}

¹ Chemistry Department, Faculty of Science, King Abdulaziz University, P.O. Box 80203, Jeddah 21589, Saudi Arabia

² Center of Excellence for Advanced Materials Research (CEAMR), King Abdulaziz University, Jeddah 21589, P.O. Box 80203, Saudi Arabia

³ Chemistry Department, Faculty of Science, Assiut University, Assiut 71516, Egypt

*E-mail: maabdo@kau.edu.sa, mahmali@aun.edu.eg; mahussein74@yahoo.com

Received: 24 May 2016 / Accepted: 5 July 2016 / Published: 7 August 2016

There is no doubt that, epoxy resin is one of the most important materials that has been widely used in coating technology. The present work is aimed to fabricate a new series of epoxy resin nanocomposites in the form of G/CNTs/EPY₁₋₄ using simple dissolution method and ultrasonic assistance. The expected nanocomposites have been fabricated using 10% loading of different mixed ratios from G/CNTs. Four different G/CNTs mixed ratios were used 20/80%, 40/60%, 60/40%, and 80/20%. The structure of the G/CNT/EPY₁₋₄ nanocomposites has been investigated and confirmed by normal characterization techniques including: X-ray diffraction (XRD), Fourier transforms infrared spectroscopy (FT-IR), Thermogravimetric analysis (TGA), Differential Thermal gravimetry (DTG) and field emission scanning electron microscopy (FE-SEM). T₂₅ and T₅₀ values for G/CNT/EPY₁₋₄ nanocomposites were slightly higher than elegant epoxy. R₅₀₀ values for the fabricated materials were in the range of 8.98 – 10.04 %. Furthermore, the role of mixed G/CNTs on the coating properties of epoxy resin was determined using electrochemical impedance and technique. The coating resistance of epoxy composites in the form of G/CNT/EPY₁₋₄ was larger than that observed for elegant epoxy coating. G/CNT/EPY₃ and G/CNT/EPY₁ showed highest and the lowest coating impedance values respectively. In addition to that, the water sorption technique has been used as a complementary method for such coating behaviour. The water uptake was efficiently decreased in all the formulations compared to the epoxy due to the presence of G/CNTs reinforcing agents.

Keywords: Epoxy resin, Mixed Graphene/Carbon nanotubes, Coating performance, Electrochemical impedance

1. INTRODUCTION

Pillions of synthetic and commercial polymers are produced long time ago and used in different branches of industry with wider applications due to their low cost, light weight and superior chemical durability, etc. [1-4]. Polymers based inorganic nano-fillers are an important type of nanocomposites which contain organic polymer as matrix and nanoparticles as nano-fillers. New efficient products are produced via this type of nanocomposites with superior properties in different fields such as engineering, environmental, electronics and fabricated devices [5-8]. Epoxy resins are ranked as important materials that have excellent coating performance and have been used over a wide range of applications. In addition to its fantastic coating properties, epoxy resins have so many additional characters and advantages that make it distinctive with multiple uses such as, its low cost, easy processing and fabrications, excellent dimensional stability, great mechanical properties and high thermal stability [9 - 13]. Meanwhile, epoxy resins are also exceedingly used in automobile, electronics and aerospace industries dearly the same advantages and properties [14 - 16]. As well as modified epoxy resins have great chemical and electrical properties in addition to the previously mentioned properties. Although, all of these advantages epoxy resins still have limited usage in microelectronic packaging due to its fundamental low thermal conductivity. Addition of nano-fillers in the form of nanoparticles to epoxy resins in the form of nanocomposites give rise to extra enhancement of properties and most of the time give additional character that appear for the first time and are not distinguished before. The new enhanced properties depends on the nature of nano-fillers that loaded within the epoxy matrices. However, homogeneous squander of reinforced nano-fillers via correct and compatible nanocomposite fabrication is consider as an important factor to ensure from such amended properties. Huge number of nanoparticles have been used as nano-fillers in the presence of epoxy resins including: Nickel lanthanum ferrites, clay, silica, zirconia, carbon nanotubes, graphene and grapheme oxide [17- 26]. Much more attention has been given to graphene and carbon nanotubes. Therefore, the suggested work is aimed to fabricate new nanocomposite materials based on epoxy resin and different loading ratios of G/CNTs. The new materials have been fabricated with the help of ultrasonic assistance for short prod of time. X-ray diffraction (XRD), Fourier transforms infrared spectroscopy (FT-IR), and field emission scanning electron microscopy (FE-SEM) have been all used to investigate and to confirm the structures of these new materials. As well as, the new G/CNTs/epoxy resin nanocomposites have been characterized using Thermogravimetric analysis (TGA) and Differential Thermal gravimetry (DTG) characterization techniques. Furthermore, detailed electrochemical study for the new fabricated materials has been considered using electrochemical impedance technique and water sorption. The role of mixed G/CNTs ratios on the properties of epoxy resin specially coating property has been also examined using such study.

2. EXPERIMENTAL

2.1. Materials, solvents and reagents:

Epikote-1001 x-75 % (2642) epoxy was utilized as commercially available epoxy resin along with crayamid – 100 % (2580) epoxy hardener and used as received without further purification. Both

compounds were used together as a matrix material in fabrication process for different compositions. The mixture ratio of 1 : 1 weight by weight was prepared from Epikote : crayamid for processing and fabrications. Chloroform of spectroscopic grade was purchased from Merck, and also used without further purification. Multi-walled carbon nanotubes (CNTs), with an average diameter of (110.0 – 170.0) nm was purchased from Sigma-Aldrich and was used as received without any purification. Graphene (G) was also purchased from Sigma-Aldrich and was also used as extradited. All other solvents and / or fragments were of high purity and were used as extradited.

2.2. Pure epoxy resin preparation:

The pure epoxy resin was prepared using simple dissolution method and ultrasonic assistance as reported in the literature [17, 18] as the following: equal amounts from Epikote-1001 and crayamid hardener epoxy using (weight: weight) ratio were used to prepare epoxy matrix and dissolved in suitable amount of chloroform. Each sample was sonicated for 5 min, then mixed together. The new mixture was further sonicated for 15 min and then poured in to Petri dish for solvent evaporation for at least 24 h at room temperature. The pure epoxy thin film was separated out and dried in the oven.

2.3. G/CNTs/epoxy resin nanocomposites preparation:

A new class of G/CNTs/epoxy resin nanocomposites was also fabricated using simple dissolution method and ultrasonic assistance. The suggested nanocomposites including a fixed weight of epoxy resin and different mixed ratios of G/CNTs (wt by wt %) is taking into account, hence the total ratio of this mixture is 10% with respect to epoxy resin matrix. Four different G/CNTs mixed ratios were used: 20/80%, 40/60%, 60/40%, and 80/20%. In a typical manner our targeted nanocomposites were fabricated as follows: while epoxy resin was prepared, different G/CNTs mixed ratios were added and scattered in to the Epikote-1001 matrix and sonicated for 5 min. An equal amount of crayamid hardener was added and the total mixture was further sonicated for 15 min. Final products in the form of thin film were produced by solvent evaporation in Petri dishes for at least 24 h at room temperature.

Table 1. Chemical compositions for G/CNTs/epoxy nanocomposites G/CNT/EPY₁₋₄

Sample	G %, (Weight, g)	CNTs %, (Weight, g)
Pure epoxy	---	---
G/CNT/EPY ₁	20%, (0.04)	80%, (0.16)
G/CNT/EPY ₂	40%, (0.08)	60%, (0.12)
G/CNT/EPY ₃	60%, (0.12)	40%, (0.08)
G/CNT/EPY ₄	80%, (0.16)	20%, (0.04)

Then dried in the oven at temperatures of 50 - 60 °C. The expected chemical compositions for G/CNTs/epoxy resin nanocomposites were illustrated in Table 1.

2.4. G/CNTs/epoxy resin nanocomposites fabricated electrodes:

G/CNTs/epoxy resin electrodes were fabricated as working electrodes using G/CNTs/epoxy resin nanocomposites and in the presence of stainless steel sheets with dimensions of 1 x 1 cm². The desired nanocomposites were prepared as described in the previous section and before final casting step. The epoxy composite mixtures in chloroform were delivered in a drop wise manner onto the stainless steel sheet to perform good examples for modified electrodes. These electrodes were cured overnight and then dried in the oven for 2 - 4 hrs at temperatures of 50 - 60 °C. The working electrodes were fabricated different times, each time using different mixed ratio from G/CNTs.

2.5. Instrumentation

FT-IR spectra were examined by using ATR smart part technique in the wave number range 4000-400 cm⁻¹ using Thermo-Nicolet-6700 FT-IR spectrophotometer. Powder X-ray diffractograms were determined in the 2θ range from 10 to 80° with the aid of Philips diffractometer (type PW 103/00) using the Ni-filtered CuK α radiation. The surface morphology was characterized by Field Emission Scanning Electron Microscope (JEOL JSM-7600F, Japan). The FE-SEM samples were prepared by evaporating a dilute solution of each nanocomposite on a smooth surface of aluminum foil, and subsequently coating it with gold palladium alloy. The microscope was operated at an accelerating voltage of 2.0 kV and 10 mm work distance carbon film. Thermal analysis, the TGA curve was recorded with a TA instrument apparatus model TGA-Q500 using a heating rate of 10 °C min⁻¹ under nitrogen atmosphere. The average masses of the samples were 5 mg. Gravimetric method was used to determine the water uptake of the different epoxy coatings. The fabricated samples were immersed in 0.1M NaCl solution for intervals of time. Electrochemical impedance spectroscopy (EIS) was recorded using a potentiostat of type Auto lab PGSTAT30, coupled to a computer equipped with FRA software. A three electrode arrangement was used, consisting of an Ag/AgCl reference electrode, a platinum counter electrode and the fabricated epoxy coated stainless steel (exposed surface area 3 cm² and 100 μ m thickness layer) as working electrode and immersed in 0.1M KCl solution. The working electrode was fabricated different times, each time using different mixed ratio from G/CNTs. EIS measurements were conducted potentiostatically at open circuit potential (E_{cor}) with 10 mV rms with frequency range 50 kHz to 0.1 Hz.

3. RESULTS AND DISCUSSION

There is no doubt that, epoxy resins are ranked as important materials that have excellent coating performance and have been used over a wide range of applications. More particularly,

modified epoxy resins have great chemical properties. Nevertheless, all of these success for epoxy resin coating performance the scientists still look for superior performance. Such expected behavior may come by appending of nanoparticles and / or mixed nanoparticles as reinforced nano-fillers to the epoxy matrix to rise up its coating ability. In addition to that, it may take out supplementary character that may be submitted for the first time. Therefore, new designed G/CNT/EPY₁₋₄ nanocomposites are fabricated in this paper by ultrasonic assistance in order to study the role of mixed G/CNTs ratios on the coating performance of the pure epoxy resin. This study is carried out using electrochemical impedance technique. Before attempting this study, the chemical structure of these new formulations is confirmed and investigated using various characterization tools. FT-IR, XRD, thermal analysis, FE-SEM measurements and water uptake are utilized and studied in details. Furthermore, the coating properties of epoxy resin is further confirmed by water sorption as a complementary test. At the end, it will be easy to determine the optimum formulation from these new nanocomposites, which will have more enhanced effect on the coating performance of pristine epoxy.

3.1. G/CNTs/epoxy resin nanocomposites characterization techniques

Different techniques are used to characterize and to identify the chemical structure for the suggested composite materials. FT-IR measurement is one of the important testimonies for composites fabrication. A obvious declaration for bonding interaction designed between neat epoxy and G/CNTs nanofillers is predestined.

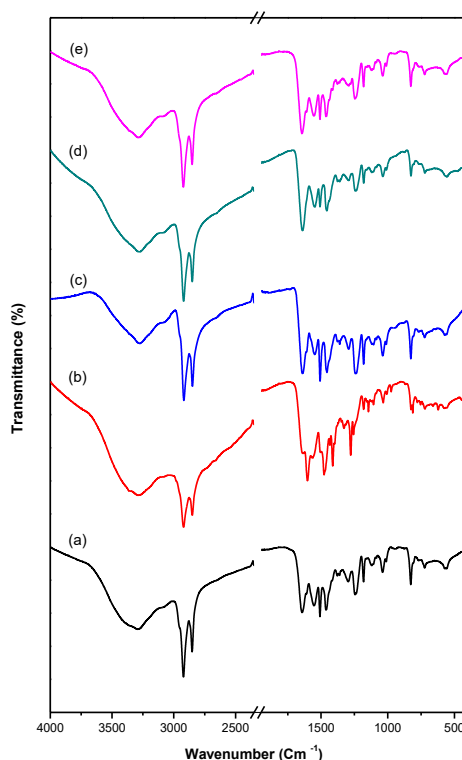


Figure 1. FT-IR spectra of (a) elegant epoxy resin, (b) G/CNT/EPY₁, (c) G/CNT/EPY₂, (d) G/CNT/EPY₃, (e) G/CNT/EPY₄.

Figure 1 shows the FT-IR spectroscopic analysis for the elegant epoxy as well as for G/CNT/EPY₁₋₄ nanocomposites over the range of 4000 to 400 cm⁻¹. The spectra show the characteristic absorption bands for epoxy and mixed G/CNTs ratios nanofillers as well. The results also show that the epoxy resin is physically combined with the reinforced G/CNTs nanofillers in all formulations. The major epoxy characteristic bands are found in the IR spectrum. Band at 3060 -3012 cm⁻¹ due to the valent CH vibrations of the epoxy ring (ν_{CH}), at about 3039 cm⁻¹ are caused by the stretching CH vibration of the aromatic ring, bands at 2924 cm⁻¹ is due to the stretching vibration of the -CH₂ functional group. In addition, bands at 1240 cm⁻¹ for the valent CO vibrations of the epoxy ring (ν_{CO}), and at 920 - 811 cm⁻¹ for the bending CH vibrations of the epoxy ring (ν_{CH}). All of these adsorption bands can also be monitored in the spectra of the all synthesized nanocomposites. Furthermore, Figure 1 shows the characteristic bands related to G and CNTs in the spectra of our new nanocomposites, which confirm such type of interaction [27-30]. More particularly, mixed G/CNTs ratio dispersion inside the elegant epoxy matrix alter its FT-IR spectrum. A closer look to the FT-IR spectra in Figure 1 shows that, the intensity of all the bands which are related to reinforced nanofillers is clearly increased with increasing the loading percentage along the composites formation. Unlike this, a considerable decrease of all characteristic epoxy bands intensities is detected in all fabricated forms of G/CNTs/epoxy composites [17].

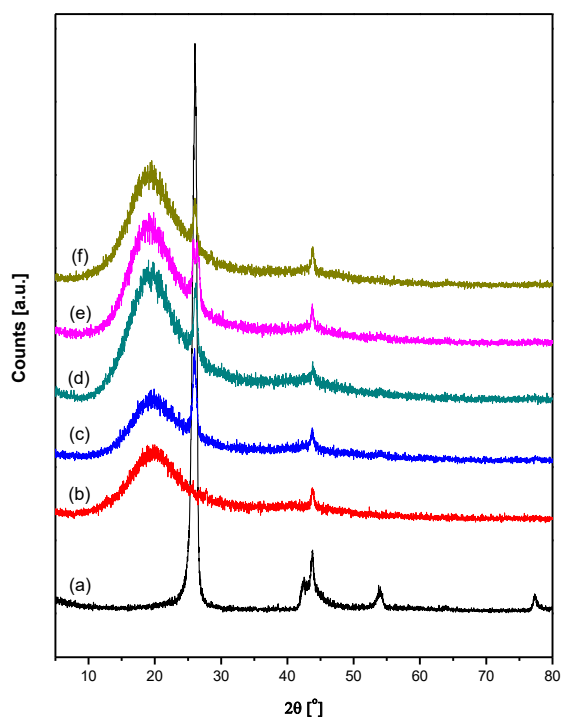
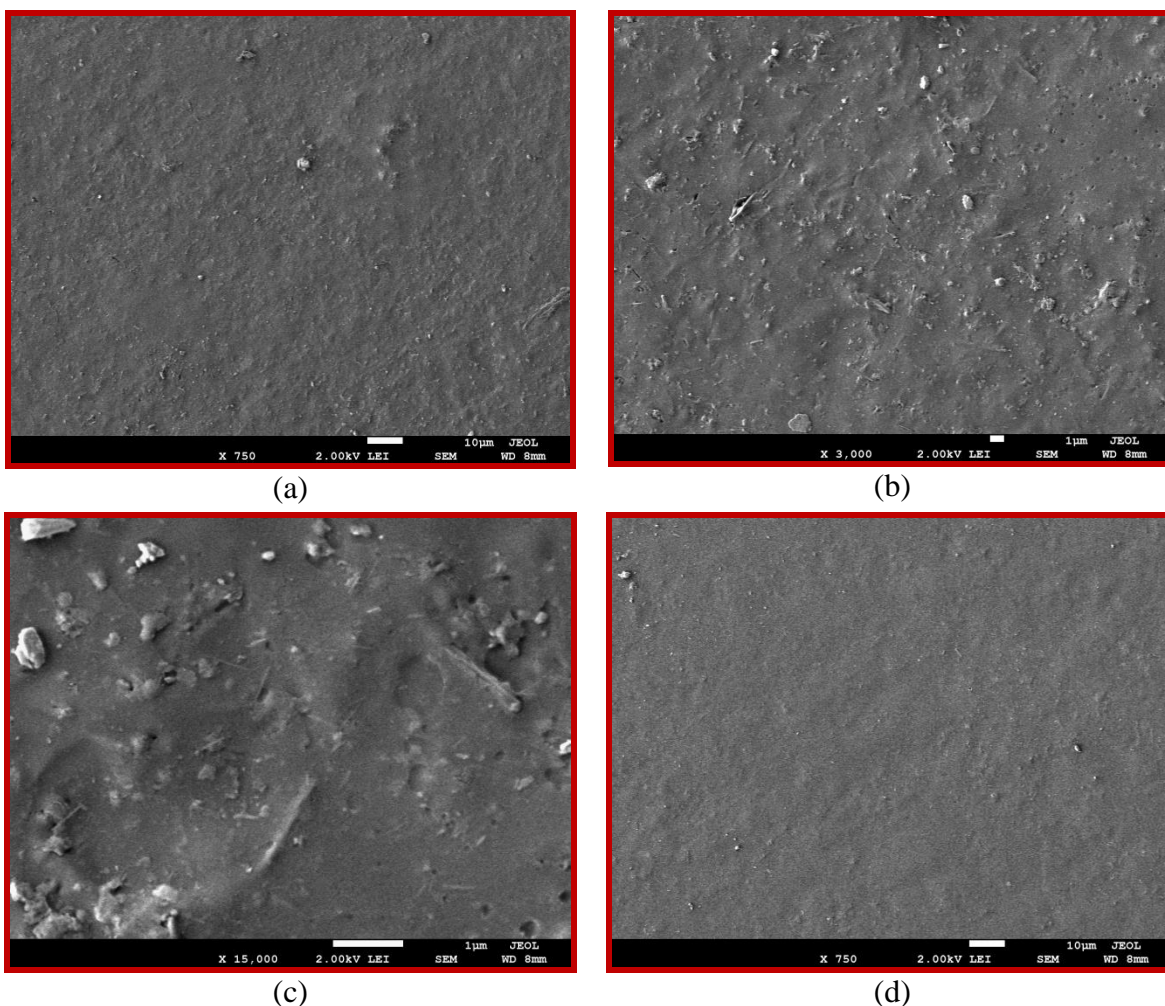


Figure 2. XRD diffraction patterns of (a) mixed G/CNTs, (b) elegant epoxy resin, (c) G/CNT/EPY₁, (d) G/CNT/EPY₂, (e) G/CNT/EPY₃, (f) G/CNT/EPY₄.

The X-ray diffractograms for the mixed G/CNTs ratio, elegant epoxy resin and our targeted G/CNT/EPY₁₋₄ nanocomposites are displayed in Figure 2.

The XRD patterns indicate that the pure epoxy and G/CNTs mixed ratios are physically joined through the expected nanocomposite formation. These XRD patterns are measured over the range of $2\theta = 5^\circ - 80^\circ$. The 2θ scan shows perfect XRD diffraction patterns for G/CNTs mixed ratio as well as elegant epoxy matrix which are in agreement with these literature data as illustrated in Figure 2_a and 2_b respectively. The XRD pattern for G/CNTs mixed ratio is given in Figure 2_a and shows a strong diffraction peak at $2\theta = 26.25^\circ$ (002) which is attributed to the graphite plane. Of course this is due to both G and CNTs nanoparticles are considered as carbon origin material. Another weak peaks appeared nearly in the range of $2\theta = 42.86^\circ - 45.8^\circ$ and $2\theta = 53.5^\circ - 54.6^\circ$ with two maxima at $2\theta = 43.7^\circ$ and $2\theta = 53.98^\circ$ respectively; in addition to very small peak at $2\theta = 77.29^\circ$ [31,32]. The major characteristic peaks are also mentioned in the XRD pattern for G/CNT/EPY₁₋₄ nanocomposites as shown in Figure 2_{c-f}. Furthermore, the XRD pattern for pure epoxy resin shows amorphous characteristic diffraction peaks as reported in the literature [17, 18, 33] which are due to the amorphous nature of the pure epoxy resin. The first peak is appeared in the range of $2\theta = 10.4^\circ - 30.8^\circ$ with a maximum at around $2\theta = 20^\circ$, besides it is wide and somewhat strong. However the second amorphous peaks are weakened and located in the range of $2\theta = 43.4^\circ - 45^\circ$ with maximum at around $2\theta = 43.7^\circ$, whoever, the third peak is very week and did not mentioned in this XRD pattern. More particularly, Figure 2_{c-f} shows the XRD diffractograms for G/CNT/EPY₁₋₄ nanocomposites.



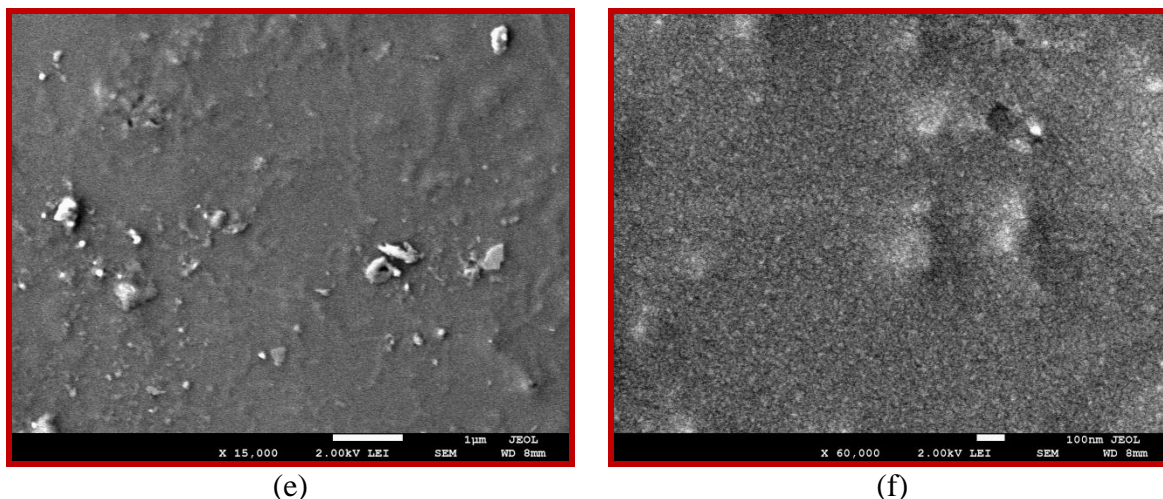


Figure 3. FE-SEM micrographs for G/CNT/EPY₁ (a) $x = 750$, (b) $x = 3000$, (c) 15000 and for G/CNT/EPY₄ (d) $x = 750$, (e) $x = 3000$, (f) 60000.

The estimated data show peaks characterizing both mixed G/CNT and pure epoxy as well in its original place without any shift. More screening of Figure 2_{c-f} exposes also without any hesitation the formation of our targeted nanocomposites. In addition there is no other crystalline bands that may be assigned to another phases or existence of dirtiness have been conducted into the desired nanocomposites.

The surface behavior of G/CNT/EPY₁₋₄ nanocomposites is estimated by using field emission scanning electron microscopy micrographs as shown in Figure 3. This study gives another clear directory for the composite formations which are mainly concentrated on the modifications that are found on the surface of each tested sample referring to its original shape. The FE-SEM samples were prepared by evaporating a dilute solution of each nanocomposite on a smooth surface of aluminum foil, and subsequently coating it with gold palladium alloy. The microscope was operated at an accelerating voltage of 2.0 kV and 10 mm work distance carbon film. The produced micrographs show considerable surface modifications due to the immersion of G/CNTs mixed nanofillers into the pure epoxy matrix. Figure 3a-c shows the surface of G/CNT/EPY₁ nanocomposite as selected example at three different magnifications $x = 750$, 3000 and 15,000. The mixed fillers are distributed in a uniform way with excellent interaction with epoxy matrix in all magnifications, which appears as accumulative globular particles in the magnification of $x = 43,000$. Whereas, FE-SEM images of G/CNT/EPY₄ nanocomposite surface as another selected example are exhibited in Figure 3_{d-f} with two similar magnifications of ($x = 750$ and 3,000) to the previous sample. A closer view to SEM images, it is clearly to say that the enforced nanofillers is also uniformly encapsulated and established inside epoxy matrix. Whoever, a good cohesion between this filler particles and polymer matrix is also observed. As well as, the images also show higher compatibility and good distribution of nanofillers in both magnifications. Furthermore, the SEM image (Figure 3_f) shows accumulative globular particles that are point out the graphene nanoparticles that are found in high percentage within G/CNT/EPY₄ formulation at very high magnification $x = 60,000$.

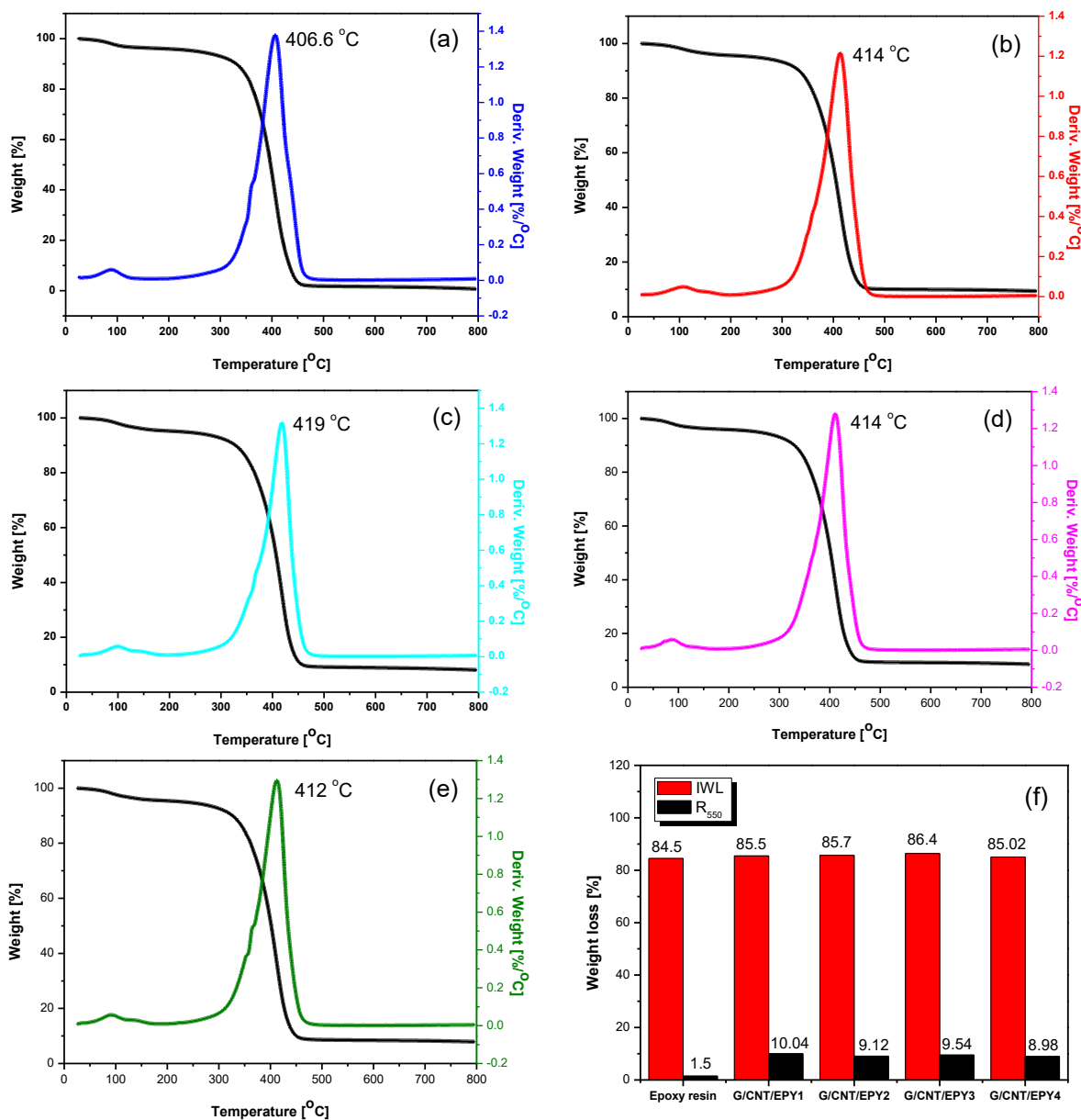


Figure 4. TGA DTG curves for (a) elegant epoxy resin, (b) G/CNT/EPY₁, (c) G/CNT/EPY₂, (d) G/CNT/EPY₃, (e) G/CNT/EPY₄, (f) schematic diagram for IWL and R₅₅₀.

There is no doubt that, thermoplastic polymers are considered as an important stylish type of cross-linking polymers. The cross-linking degree plays a remarkable role in the thermal degradation of such polymeric type. As it is reported there is two main types of cross-linking epoxy stoichiometric and non-stoichiometric epoxy according to the presence of free amino groups or not. Both types have a significant effect on the thermal behavior of epoxy composite materials as mentioned in the literature [34 - 37]. Furthermore, the thermal stability of epoxy resin composite materials is also depending on the type of reinforced nanoparticles and its role on the epoxy structure. A lot of enjoyable manuscripts that are concentrated on this property are found in the open literature. For examples montmorillonite clay, aluminium oxide, silicon oxide and magnesium oxide enhanced thermal stability of pure epoxy [38, 39]. On the contrary, most of the transition metal oxides (CuO, ZnO, TiO₂ and oxides Mn-Zn or

Ni-Zn ferrite) act as catalysts and hence accelerate the degradation effect of the prepared epoxy resin formulations [34, 40 - 42]. Our designed epoxy is fabricated in a stoichiometric ratio as aforementioned in the experimental part. The thermal stability of epoxy resin and our targeted G/CNT/EPY₁₋₄ nanocomposites are estimated by TGA & DTG thermal analysis techniques under nitrogen atmosphere at a heating rate of 10°C min⁻¹ as illustrated in Figure 4a-f. TG values are measured from room temperatures up to 800°C.

Table 2. Thermal behavior of elegant epoxy and G/CNT/EPY₁₋₄ nanocomposites

Symbol	IWL ^{**} (%)	PDT _{max} ^{***} (°C)	R ₅₅₀ (%)	Temperature (°C) for various percentage decompositions [*]	
				T ₂₅	T ₅₀
Epoxy resin	84.50	406	1.5	368	394
G/CNT/EPY ₁	85.50	414	10.04	375.07	405
G/CNT/EPY ₂	85.7	420	9.12	378.36	406.86
G/CNT/EPY ₃	86.40	414	9.54	373.6	403.9
G/CNT/EPY ₄	85.02	412	8.98	372.4	402.2

* The values were determined by TGA at heating rate of 10°C min⁻¹

** The values were determined by TGA AT 350 °C.

*** The values were determined by DTG.

Table 2 shows the temperatures for diverse percentages of degradations. Temperatures at 25 and 50 % of weight losses are determined in the form of T₂₅ and T₅₀ respectively. The TG curves show a little weight loss within a range of 85 - 172 °C up to maximum of 5%. Such weight loss is assigned to the loss of imbibed humidity, entrapped solvents and/or water molecules [35 - 37]. The curves also indicate that all composites as well as epoxy resin decompose in one step. the decomposition is very fast during this step for all sample with a small shift of the temperatures toward higher values in case of G/CNT/EPY₁₋₄ comparing with pure epoxy. The decomposition starts at nearly 342 °C for the elegant epoxy and is completed at nearly 468 °C, whereas, G/CNT/EPY₁₋₄ decompose in the range of 350 - 485 °C. The predictable nature of degradation in this step is related to decomposition of the resin into lower molecular weight fragments as side products [37, 38]. The initial weight loss % (IWL) is referring to the observed weight loss at 350 °C. No significant decomposition are mentioned before IWL in all fabricated G/CNT/EPY₁₋₄. Pure epoxy shows 84.5% IWL value which is consider the lowest value; while G/CNT/EPY₁₋₄ show IWL values in the range 85.02 – 86.40 % as shown in Figure 4f. G/CNT/EPY₄ shows the lowest IWL value G/CNT/EPY₃ shows the highest value; which is referring to the relative higher and lower stability of both products respectively.

G/CNT/EPY₁₋₄ nanocomposites show slight increase for T₂₅ and T₅₀ compared to the elegant epoxy. Of course it is not significant considerable increase, but according to our reports in the previous studies the obtained results could be consider as good enough to start to find a way in order to increase the thermal stability of epoxy resin composites. Nanofillers in the forms of NiLa_xFe_{2-x}O₄ (x = 0.00 – 2.00) and Ni-La-Ferrites are found to be like good catalysts to expedite the thermal degradation for the epoxy resin [17, 18]. G/CNT/EPY₂ display higher T_{25%} & T_{50%} values compared to the other

formulations (378.36 and 406.86 °C); whereas, G/CNT/EPY₄ display lower values (372.4 and 402.2 °C). More particularly, the solid residue left at 550 °C are illustrated ad R₅₅₀. Almost nearly the same residue is found for all composites G/CNT/EPY₁₋₄, unlike the pure epoxy which is decomposed completely. Nearly 1.5 % residue is observed as a char end product from the decomposition of epoxy resin. R₅₀₀ values for the fabricated materials are in the range of 8.98 – 10.04 % as also shown in Figure 4f. To understand this behavior and as it is pointed out in the preparation method, epoxy resin with different mixed ratios of G/CNTs (wt by wt %) is prepared, taking into account the total ratio of this mixture is 10% with respect to epoxy resin matrix.

3.2. Coating performance of G/CNTs/epoxy resin nanocomposites

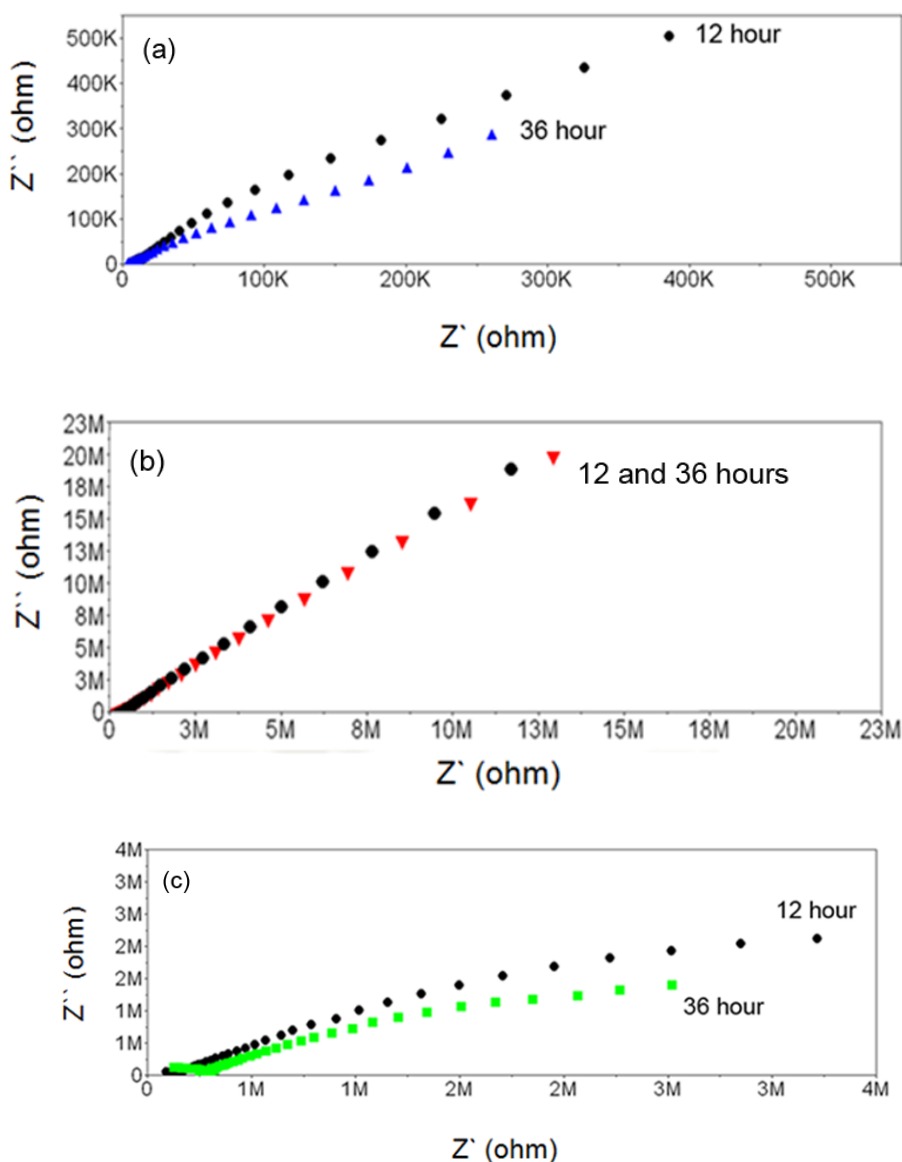


Figure 5. Electrochemical impedance spectrum for (a) elegant epoxy coating, (b) G/CNT/EPY₃, (C) G/CNT/EPY₁ after immersion time 12, 36 hours.

The coating behaviour of epoxy resin and G/CNT/EPY₁₋₄ nanocomposites is carried out by electrochemical impedance technique and water uptake as well. Detailed electrochemical study for the new fabricated materials is considered using electrochemical impedance technique. The coating performance of pure epoxy and G/CNT/EPY₁₋₄ nanocomposites is determined by electrochemical impedance technique. The tested materials are deposited on the electrode surface as a source of stainless steel substrate. The measurements are achieved within 5 days of immersion using 0.1 M solution of potassium chloride. A continuous measurements of each sample at fixed time are carried out during this period in order to obtain impedance curve which is presented by Nyquist plot [43, 44]. Figure 5a-c shows Nyquist plots of pure epoxy, G/CNT/EPY₃ and G/CNT/EPY₁ after 12 and 36 hours immersion time. Perfect covering partition layers for the stainless steel substrate in the tested aqueous potassium chloride solution are observed due to the coating capacitance at higher frequencies. G/CNT/EPY₃ shows higher coating resistance value, while G/CNT/EPY₁ demonstrates the lower value. The order of high coating resistance values compared to the elegant epoxy is given as: G/CNT/EPY₃ > G/CNT/EPY₂ = G/CNT/EPY₄ > G/CNT/EPY₁ > pure epoxy.

The pure epoxy coating impedance spectrum is observed by the coating resistance at the low frequency as illustrated in Figure 5a. The data shows a significant decrease in the measured coating resistance with increasing the time of immersion. This is of course attributed to the increase of water molecules inside the epoxy structure due to the water uptake property and hence, increase the conductivity of this coated layer [45, 46].

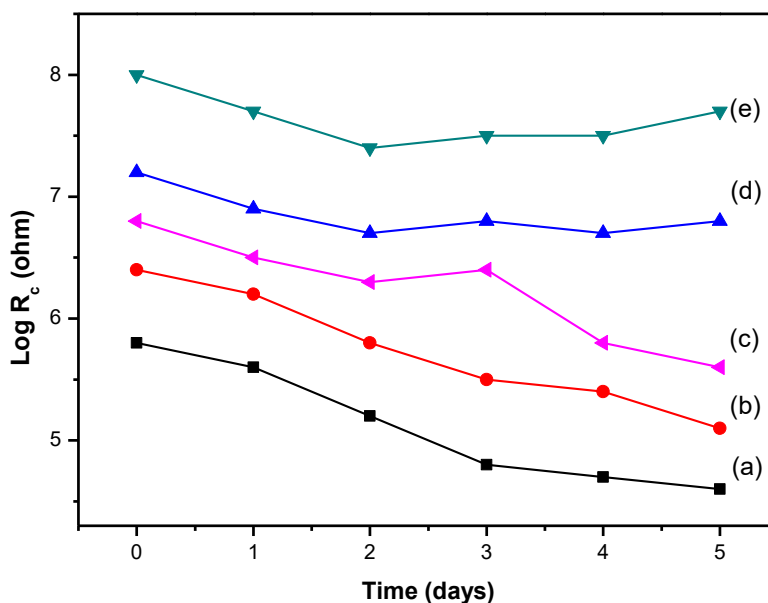


Figure 6. The change of coating resistance of different epoxy formulations with immersion time. (a) elegant epoxy resin, (b) G/CNT/EPY₁, (c) G/CNT/EPY₂, (d) G/CNT/EPY₃, (e) G/CNT/EPY₄.

Furthermore, Figure 5c, also shows a mild decrease in the measured coating resistance with increasing the time of immersion at higher frequency values. Whereas, Figure 5b shows the coating

impedance of G/CNT/EPY₃ as an excellent example to enhance the epoxy coating behavior. The data shows a large coating resistance value comparing to the observed for pure epoxy. Furthermore, No respectable change in the coating resistance is observed which is attribute to lower water uptake behavior for such composite. The loaded nanofillers act as building cores that can block the vacant spaces within the epoxy matrix which increase the coating resistance and hence reduce the water uptake ability . This observation is confirmed in the coming water sorption study. On the other hand, G/CNT/EPY₁ shows the lowest coating impedance value compared to the other formulations, whoever, this value still higher than the pure epoxy value. Other G/CNT/EPY_{2,4} show nearly analogous coating impedance values, which lying in between the previously mentioned values.

Figure 6 illustrates the changes in the coating resistance values for elegant epoxy as well as for G/CNT/EPY₁₋₄ composites with increasing the immersion time. It is obviously noticed that, the acquired results for the coating resistance values is in agreement with that discussed previously in Figure 5a-c and the gravimetric method which will discussed bellow. It is concluded that, the impedance data of our targeted epoxy resin composites coatings is roughly better than results obtained in our previous study. The G/CNTs mixed ratios are considered as superior coating nanofillers than Ni-La-Ferrite nanoparticles, which worthily enhance the coating performance of the pure epoxy.

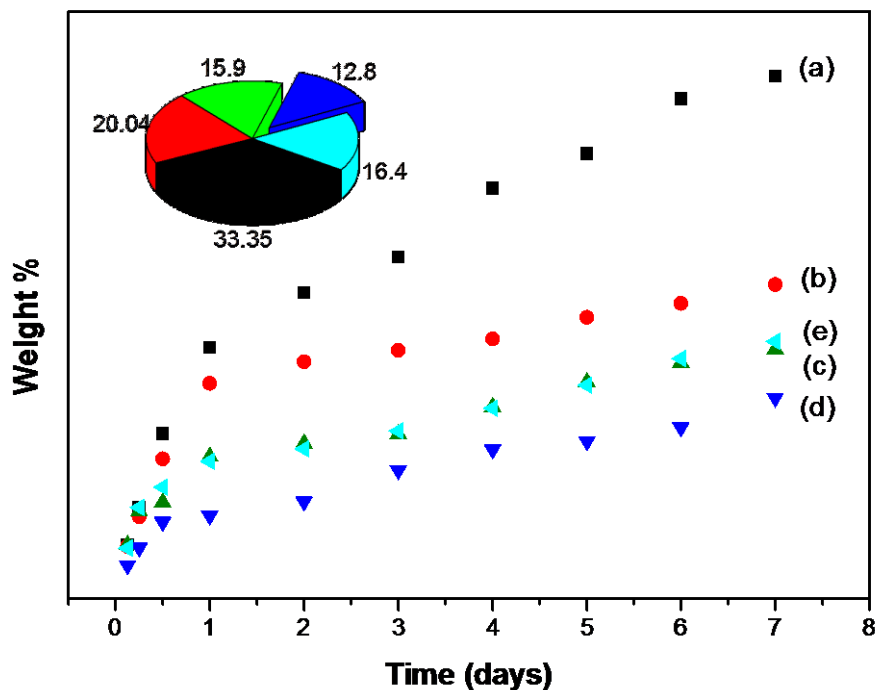


Figure 7. The perversion of water uptake for (a) Elegant epoxy, (b) G/CNT/EPY₁, (c) G/CNT/EPY₂, (d) G/CNT/EPY₃, (e) G/CNT/EPY₄ with the immersion time in days.

The sorption of water is considered as a complementary technique that is to estimated the coating behaviour of materials. Water uptake test of different modified epoxy samples G/CNT/EPY₁₋₄ nanocomposites as well as the pure epoxy is determined by well known gravimetric technique. The

fabricated samples were immersed in 0.1M KCl solution for intervals of time. The water sorption of the tested samples is defined as

$$\text{Water sorption} = \frac{W_t - W_o}{W_o} \times 100 \quad (1)$$

Where W_o and W_t are the weight of the samples before and after immersion in the prepare solution for different periods of time.

Figure 7 shows the alteration sorption of water of the elegant epoxy and G/CNT/EPY₁₋₄ nanocomposites depending on the time of immersion in days. The neat epoxy and G/CNT/EPY₁₋₄ samples are immersed for 7 days during this test. The measurements are carried out in a solution of sodium chloride at room temperature. The measuring time is a little pit fast in the first day (each 3 hours), after that the measuring time is constant once a day. The data show that, the water uptake property for all G/CNT/EPY₁₋₄ samples are sharply increased with increasing the time of immersion within the first day of measurement, then slightly increased day by day to the end of immersion time. Nearly straight lines are obtained for the points after the first day of measurements with different slopes in all G/CNT/EPY samples. G/CNT/EPY₁ shows the lowest water uptake behavior (20.04%); while G/CNT/EPY₃ shows the highest value among the tested epoxy composites (nearly 13%). More particularly, G/CNT/EPY_{2,4} show nearly similar values (15.9%) and (16.4%) respectively; these values lie between the previously mentioned values. The amount of water uptake and consequently the rate of water insertion by the pure epoxy is quite larger enough as it is reported in the literature [47, 48]. This is due to the continuous absorption of water inside the pure epoxy. Water molecules spread between epoxy chains and increase the swelling behavior. Conversely, the presence of G/CNTs as reinforcing agent in all the formulations G/CNT/EPY₁₋₄ decrease effectively the water uptake in comparison to the epoxy. Such effect is raised while the loading of G/CNTs mixed ratio is raised. This is attributed to, the blocking effect for G/CNTs nanofillers; where it is act as building cores that can block the vacant spaces within the epoxy matrix. Finally it is concluded that, the amount of water uptake is decreased with increasing the G content in the designed new formulations till G/CNT/EPY₃ then slightly increased.

4. CONCLUSIONS

Four new formulations based on epoxy resin and G/CNTs loading ratios in the form of G/CNT/EPY₁₋₄ are fabricated by simple dissolution method with the help of ultrasonic assistance. XRD, FT-IR and FE-SEM are used to investigate and to confirm the structures of these new materials. Besides that, the new G/CNTs/epoxy resin nanocomposites have been characterized using Thermal analysis characterization techniques (TGA and DTG). FT-IR spectra show that the epoxy resin is physically combined with the reinforced G/CNTs nanofillers. FE-SEM micrographs exhibit significant distribution and compatibility as well for nanofillers at different magnifications. No significant degradation are found before IWL in all fabricated G/CNT/EPY₁₋₄. G/CNT/EPY₁₋₄ show IWL values in the range 85.02 – 86.40 %. More particularly, electrochemical impedance and water sorption techniques are used to study the coating behaviour for these new fabricated materials. The role of mixed G/CNTs ratios on the coating properties of epoxy resin is estimated using both techniques. The

coating resistance of the epoxy resin was significantly improved by immersion of G/CNTs mixed ratios inside epoxy matrix. Results obtained from impedance are in accordance with that observed in water uptake.

ACKNOWLEDGEMENTS

This work was funded by the Center of Excellence for Advanced Materials Research (CEAMR), King Abdulaziz University, Jeddah under grant no. (CEAMR-SG-7-437). The authors, therefore, acknowledge with thanks CEAMR technical and financial support.

References

1. W. Dai, J.H. Yu, Y. Wang, Y.Z. Song, F.E. Alam, K. Nishimura, C.-T. Lin, N. Jiang, *J. Mater. Chem.*, A3 (2015) 4884.
2. P. K. Samantray, P. Karthikeyan, K. S. Reddy, *Int. J. Heat Mass Transfer*, 49 (2006) 4209.
3. Y.C. Zhang, K. Dai, J.H. Tang, X. Ji, Z.M. Li, *Mater. Lett.*, 64 (2010) 1430.
4. V. Datsyuk, S. Trotsenko, S. Reich, *Carbon*, 52 (2013) 605.
5. J. He, Y. Shen, D. G. Evans, X. Duan, *Composites: Part A*, 37 (2006) 379.
6. Y. Wang, N. Herron, *Science*, 273 (1996) 632.
7. T.C. Merkel, B.D. Freeman, R.J. Spontak, Z. He, I. Pinnau, P. Meakin, A.J. Hill, *Science*, 296 (2002) 519.
8. G.W. Peng, F. Qiu, V.V. Ginzburg, D. Jasnow, A.C. Balazs, *Science*, 288 (2000) 1802.
9. J. Jiao, X. Sun, T.J. Pinnavaia, *Adv. Funct. Mater.*, 18 (2008) 1067.
10. B.C. Luo, X.H. Wang, Q.C. Zhao, L.T. Li, *Compos. Sci. Technol.*, 112 (2015) 1.
11. X.F. Zhang, H.Y. Sun, C. Yang, K. Zhang, M.M.F. Yuen, S.H. Yang, *RSC Adv.*, 3 (2013) 1916.
12. J. Kong, Y.S. Tang, X.J. Zhang, J.W. Gu, *Polym. Bull.*, 60 (2008) 229.
13. J.W. Gu, Q.Y. Zhang, H.C. Li, Y.S. Tang, J. Kong, J. Dang, *Polym. Plast. Technol. Eng.*, 46 (2007) 1129.
14. A. A. Azeez, K. Y. Rhee, S. J. Park, and D. Hui, *Compos. Part B*, 45 (2013) 308.
15. S. Pavlidou and C. D. Papaspyrides, *Prog. Polym. Sci.*, 33 (2008) 1119.
16. S. C. Tjong, *Mater. Sci. Eng. R Reports*, 53 (2006) 73.
17. A. M. Asiri, M. A. Hussein, B. M. Abu-Zied, A.A. Hermas, *Compos. Part B*, 51 (2013) 11.
18. A. M. Asiri, M. A. Hussein, B. M. Abu-Zied, A.A. Hermas. *Polym. Compos.*, 36 (2015) 1875.
19. M. Behzadnasab, S.M. Mirabedini, M. Esfandeh, *Corros. Sci.*, 75 (2013) 134.
20. S.M. Mirabedini, M. Behzadnasab, K. Kabiri, *Compos. Part A*, 43 (2012) 2095.
21. T.K. B. Sharmila, A. B. Nair, B. T. Abraham, P.M. S. Beegum, E. Th. Thachil, *Polymer*, 55 (2014) 3614.
22. H.-P. Chang, H.-Ch. Liu, Ch.-S. Tan, *Polymer*, 75 (2015) 125.
23. Z. Ying, L. Xianggao, Ch. Bin, Ch. Fei, F. Jing, *Composite Structures*, 132 (2015) 44.
24. M. R. Zakaria, H. Md. Akil, M. H. Abdul Kudus, A. H. Kadarman, *Composite Structures*, 132 (2015) 50.
25. J. Jiao, L. Wang, P. Lv, Y. Cui, J. Miao *Materials Letters*, 129 (2014) 16.
26. P. Li, Y. Zheng, M. Li, T. Shi, D. Li, A. Zhang, *Materials & Design*, 89, (2016) 653.
27. A. Razzazan, F. Atyabi, B. Kazemi, R. Dinarvand, *Mat. Sci. and Eng.*, C 62 (2016) 614.
28. M. Abdel Salam, R. Burk, *Anal. Bioanal. Chem.*, 390 (2008) 2159.
29. A. T. Lawal, *Talanta*, 131, (2015) 424.
30. M. Naebe, J. Wang, A. Amini, H. Khayyam, N. Hameed, L. H. LI, Y. Chen, B. Fox, *Scientific reports*, 4, (2014) 4375.
31. W. Feng, F. Zhou, X. Bai, J. Liang, X. Wang, K. Yoshino, *Jpn J Appl Phys.*, 42, (2003) 5726.

32. R.M. Mohamed, M Abdel Salam, *Mat. Res. Bull.*, 50, (2014) 85.
33. K. H. Ding, G. L. Wang, M. Zhang, *Mat. and Design.*, 32 (2011) 3986.
34. M.S. Boon, W.P. Serena Saw, M. Mariatti, *J Mag. and Mag. Mat.*, 324 (2012) 755.
35. Z. Brito, G. Sánchez, *Composite Structures*, 48 (2000) 79 .
36. S-J. Park, F-L. Jin, *Polym. Deg. and Stab.*, 86 (2004) 515.
37. B.K. Kandola, B. Biswas, D. Price, A.R. Horrocks, *Polym. Deg. and Stab.*, 95 (2010) 144.
38. M.S. Lakshmi, B. Narmadha, B.S.R. Reddy, *Polym. Deg. and Stab.*, 93 (2008) 201.
39. B. Guo, D. Jia, C. Cai, *Eur. Poly. J.*, 40 (2004) 1743.
40. S.C. Liufu, H.M. Xiao, Y.P. Li, *Polym. Deg. and Stab.*, 87 (2005) 103.
41. Z.H. Guo, X.F. Liang, T. Pereira, R. Scaffaro, H.T. Hahn, *Composites Science and Technology*, 67 (2007) 2036.
42. P.C. Chiang, W.Z. Whang, *Polymer*, 44 (2003) 2249.
43. M. Behzadnasab, S.M. Mirabedini, K. Kabiri, S. Jamali, *Corr. Sci.*, 53 (2011) 89.
44. Y. Liu, J. Wang, L. Liu, F. Wang, Y. Li, F. Wang, *Corr. Sci.*, 74 (2013) 59.
45. M. Niknahad, S. Moradian, S.M. Mirabedini, *Coros. Sci.*, 52 (2010) 1348.
46. M. Behzadnasab, S.M. Mirabedini, K. Kabiri, S. Jamali, *Corros. Sci.*, 53 (2011) 89.
47. P. Boinard, W.M. Banks, R.A. Pethrick. *Polymer*, 46 (2005) 2218.
48. S. Morsch, S. Lyon, S.D. Smith, S.R. Gibbon. *Progress in Organic Coatings*, 86 (2015) 173.

© 2016 The Authors. Published by ESG (www.electrochemsci.org). This article is an open access article distributed under the terms and conditions of the Creative Commons Attribution license (<http://creativecommons.org/licenses/by/4.0/>).